International Journal of Nanomedicine

Dovepress
open access to scientific and medical research

Open Access Full Text Article

ORIGINAL RESEARCH

Suppression of NLRP3/Caspase-1/GSDMD Mediated Corneal Epithelium Pyroptosis Using Melatonin-Loaded Liposomes to Inhibit Benzalkonium Chloride-Induced Dry Eye Disease

Qi Lou[1,*], Lu Pan[1,*], Shengjin Xiang[1,2,*], Yueting Li[1], Jiahui Jin[1], Jingyang Tan[1], Baoshan Huang[1,2], Kaihui Nan[1,2], Sen Lin[1,2]

[1]National Engineering Research Center of Ophthalmology and Optometry, School of Biomedical Engineering, Wenzhou Medical University, Wenzhou, 325027, People's Republic of China; [2]State Key Laboratory of Ophthalmology, Optometry and Vision Science, School of Ophthalmology & Optometry, Wenzhou Medical University, Wenzhou, 325027, People's Republic of China

*These authors contributed equally to this work

Correspondence: Kaihui Nan; Sen Lin, School of Ophthalmology & Optometry and Eye Hospital, Wenzhou Medical University, Wenzhou, 325027, People's Republic of China, Tel +86-577-88067962, Email lin_sen@wmu.edu.cn; nankh@163.com

Introduction: Benzalkonium chloride (BAC) is widely employed as a preservative in eye drops, which will cause the death of corneal epithelial cells due to ROS production, DNA strand breakage, and mitochondrial dysfunction, resulting in dry eye disease (DED)-like changes in ocular surface tissues. In this study, Melatonin (MT) liposomes (TAT-MT-LIPs) designed by loading MT into TAT-modified liposomes have been developed, characterized, and used for inhibiting BAC-induced DED (BAC-DED).

Methods: The TAT was chemically grafted onto the Mal-PEG_{2000}-DSPE by Michael's addition between the sulfhydryl group in TAT and the maleimide group in Mal-PEG_{2000}-DSPE. TAT-MT-LIPs were prepared using film dispersion followed by the extrusion method and topically treated in rats once a day. BAC-DED was induced in rats by topical administration with 0.2% BAC twice daily. Defects, edema, and inflammation of the corneas, as well as IOP, were examined. Histologic analyses of corneas were performed to assess the change of mitochondrial DNA oxidation and NLRP3/Caspase-1/GSDMD signaling transduction.

Results: After topical administration, TAT-MT-LIPs significantly alleviated DED-clinical symptoms of experimental animals by inhibiting tissue inflammation and preventing the loss of the corneal epithelium and conjunctival goblet cells. Our data suggested continuous ocular surface exposure of BAC-induced NLRP3/Caspase-1/GSDMD mediated corneal epithelium pyroptosis, which was not reported before. BAC caused substantial mt-DNA oxidation, which promoted the transduction of NLRP3/Caspase-1/GSDMD and consequent corneal epithelium pyroptosis. TAT-MT-LIPs could efficiently suppress the BAC-induced corneal epithelium pyroptosis and inflammation by inhibiting mt-DNA oxidation and the subsequent signal transmission.

Conclusion: NLRP3/Caspase-1/GSDMD mediated corneal epithelium pyroptosis is involved in the development of BAC-DED. The present study provided new insights into the adverse effects of BAC, which can serve as a new target for protecting corneal epithelium when applying BAC as a preservative in eye drops. The developed TAT-MT-LIPs can efficiently inhibit BAC-DED and give great potential to be developed as a new DED treatment.

Keywords: melatonin liposome, dry eye disease, benzalkonium chloride, pyroptosis, NLRP3/Caspase-1/GSDMD signaling axis

Introduction

Benzalkonium chloride (BAC) is widely employed as a preservative in eye drops.[1] Increasing pieces of evidence have proved that consistent exposure to BAC causes dry eye disease (DED)-like changes in ocular surface tissues (eg, corneal epithelium defect, conjunctival goblet cell loss, tear film instability, and persistence ocular surface inflammation),[2–4] nevertheless the mechanism underly is still largely unclear. DED is the leading ocular surface disease in morbidity in

Received: 4 January 2023
Accepted: 3 May 2023
Published: 9 May 2023

ophthalmic clinics,[5] which affects up to 30% of worldwide populations.[6] Tear film hyperosmolarity and tissue inflammation are generally recognized as critical risk factors in DED.[7] Tear film hyperosmolarity induces the overproduction of reactive oxygen species (ROS), which leads to continuingly oxidative damage to the bio-molecules (DNA, proteins, and lipids) and causes ocular surface inflammation.[8] The inflammation in the ocular surface improves the evaporation of tear, which aggravates tear film hyperosmolarity and generates additional tissues inflammation (namely as the "vicious cycle of inflammation").[9] Zheng et al have observed on a dry eye animal model and a hypertonic cell (human corneal epithelial cells) model that the ROS in corneal epithelium enhanced the expression (both gene and protein level) of pyrin domain (PYD)-containing protein 3 (NLRP3) and promoted the secretion of IL-1β which results in ocular surface inflammation.[5,9] Noteworthily, activation of NLRP3 inflammasome can also encourage the proteolytic cleavage of gasdermin D (GSDMD) to execute pyroptotic cell death by stimulating the activation of caspase-1, caspase-4, caspase-5, or caspase-11.[10–13] Multifarious stimulus are involved in the activation of the NLRP3 inflammasome, including ROS production, chloride ion (Cl^-) efflux, and mitochondrial dysfunction, thus as a consequence of pyroptosis.[11,14–16] BAC can induce ROS production, DNA strand breakage, and mitochondrial dysfunction, leading to the death of corneal epithelial cells.[4,17] Therefore, we postulate that pyroptotic cell death induced by NLRP3 inflammasome activation may be involved in corneal epithelium loss under BAC-induced DED (BAC-DED) and suppression of pyroptosis and inflammatory factor secretion by effective scavenging of mitochondrial ROS using an ocular-surface-long-lasting antioxidant-liposome may give unexpected therapy effects against BAC-DED.

Melatonin (MT), N-acetyl 5-methoxy-tryptamine, is a potent antioxidant with a variety of physiological and metabolic advantages, including regulating circadian rhythm, anti-inflammatory and adjusting immune reaction.[18,19] It exerts antioxidant activity by scavenging ROS and reactive nitrogen species (RNS), and controlling the bioactivity of oxidation-reduction enzymes.[18] More importantly, MT is preferably distributed in mitochondria after being internalized by cells, thus acting as an effective mitochondrial ROS scavenger.[20–22] It has been locally administrated to treat oxidative stress-related retina disease (eg, age-related macular degeneration, retinopathy),[23,24] and topically applied to inhibit DED.[25,26] Otherwise, MT exhibits various robust capacities, including inhibition of NLRP3 inflammasome, attenuation of pyroptosis, and interception of inflammatory factor secretion,[27–29] thus it may show incredible ability in protection of corneal epithelium against BAC-DED. In the case of ocular surface medication, the alternatingly hydrophilic/hydrophobic structure of tear film, tightly connected lamellar structures of the cornea, and the physiological activities of an eye (blinking, tear circulation, nasolacrimal drainage) rapidly eliminated the drug from eye surface, which together-constitute the significant barriers that dramatically lowered the bioavailability of the drug.[30,31] With appropriate modifications, nanostructures including nano-micelles, liposomes, and nanogel have been extensively investigated to overcome these onsite barriers.[26,32–34] Liposome-based nanocarriers have been approved by Food and Drug Administration (FDA) for clinical uses, which are able to encapsulate both hydrophilic and hydrophobic drugs in their core and shell, respectively.[35,36] Moreover, cell-penetrating peptides (CPPs) have been widely applied to mediate the trans-barriers of drug delivery.[37,38] Specifically, the trans-activator of transcription (TAT) fragment, one of CPPs derived from human immunodeficiency virus 1 with an amino-acid sequence of NH_2-YGRKKRRQRRR-COOH, has been employed to facilitate the delivery of proteins, nucleic acids, small molecules, and nanocarriers by overcoming several types of biological barriers.[39,40]

In this study, MT liposomes (TAT-MT-LIPs) designed by loading MT into TAT-modified liposomes have been developed and characterized. The effects of TAT on the physicochemical properties and biological effects (cell uptake, therapeutic effects) of TAT-MT-LIPs were investigated. After topical administration, the therapeutic effects of MT-LIPs against BAC-DED were evaluated. What is noteworthy is that the effects of NLRP3/Caspase-1/GSDMD mediated corneal epithelium pyroptosis on the development of BAC-DED were characterized. While effectively delivering MT by TAT-modified liposomes can acquire excellent therapy effects against BAC-DED by suppressing pyroptosis and tissue inflammation in corneal epithelium. Since BAC is widely employed as a preservative in eye drops, the present study can benefit DED therapy by providing new insights into the adverse effects of BAC and a novel formula to inhibit BAC-DED.

Materials and Methods

Materials and Reagents

Hydrogenated soybean phospholipids (HSPL) and cholesterol were purchased from Macklin Reagents (Shanghai, China). Melatonin and coumarin-6 were purchased from Aladdin Reagents (Shanghai, China). The 1,2-distearoyl-sn-glycero -3-phosphoethanolamine-N-[maleimide(polyethyleneglycol)-2000] (Mal-PEG_{2000}-DSPE) was purchased from Ponsure Biotechnology (Shanghai, China). TAT (Cys-AYGRKKRRQRRR) was purchased from Apepetide (Shanghai, China). Benzalkonium chloride (BAC) was purchased from Sigma-Aldrich (USA). PAS staining solution (glycogen staining solution) was bought from Phygene. Anti-DNA/RNA damage antibody was purchased from Abcam (USA). NLRP3 polyclonal antibody was purchased from Gene Tex (USA). IL-1β polyclonal antibody, caspase 1/p20/p10 polyclonal antibody, and GSDMD polyclonal antibody were purchased from Protein tech (Wuhan, China). The HCECs cell line (human immortalized corneal epithelial cells) was purchased from Beijing Beina Chuanglian Biotech Cell Repository (BNCC, China).

Animals

Healthy SD rats (6–8 weeks old and the average weight was 180–200 g) were provided by the Experimental Animal Center of Wenzhou Medical University (the license number of experimental animals: syxk (ZheJiang) 2010–0150, in line with the experimental standard). The experiments were approved by the animal experiment ethics committee of Wenzhou Medical University. Animal welfare and experimental procedures have complied with the principles of Laboratory animal-Guidelines for the ethical review of animal welfare in China (GB/T 35892–2018).

Synthesis of TAT-PEG_{2000}-DSPE

The TAT-PEG_{2000}-DSPE was synthesized using the method described previously.[41] Briefly, Mal-PEG_{2000}-DSPE and TAT were dissolved and mixed in a chloroform/methanol (1:1, v/v) solution. The mixture was reacted under stirring at room temperature for 36 h under a nitrogen atmosphere. The obtained TAT-PEG_{2000}-DSPE was purified through rotary evaporation, following ultra filtering (molecule weigh cut-off (MWCO) 3000 Da, centrifugation at 4000 rpm) to remove the un-reacted TAT and eventually re-dissolved in PBS. The molecule structure of TAT-PEG_{2000}-DSPE was identified by ^{1}H-NMR (400 MHz, German Bruker).

Preparation of MT-LIPs and TAT-MT-LIPs

The MT-LIPs were prepared by film dispersion followed by the extrusion method.[42] Specifically, HSPL (10 mg/mL) and cholesterol (1 mg/mL) were dissolved in chloroform separately and sonicated till dissolved. The MT was dissolved in ethanol at 1 mg/mL. The HSPL-, cholesterol-, and MT-solution were mixed in a glass tube at ratios upon the experimental design. A thin film was formed at the bottom of the tube with nitrogen treatment to remove the solvents. The liposomes were obtained by dispersing this thin film in PBS buffer and hydrated for 2 h under sonication. To enhance their uniformity, we repeatedly manual-extruded the liposome suspensions to pass through the polycarbonate membranes (pore size 0.2 μm) for 10 cycles using an Avanti mini-extruder (Merck). The TAT-modified liposome was prepared using the same method, except that TAT-PEG_{2000}-DSPE partly replaced the HSPL at the designed proportion.

Characterization of TAT-MT-LIPs and MT-LIPs

The hydrodynamic diameter, zeta potential, and polydispersity index (PDI) of liposomes were analyzed by ZS-90 Zetasizer (Malvern Instruments, UK). The morphologies of MT-LIPs and TAT-MT-LIPs were observed under a transmission electron microscope (TEM, JEM-1230, JEOL, Japan).

The entrapment capacity of liposome for MT was determined using the method described previously,[43] with some modifications. After loading into liposomes, the entrapped and un-entrapped MT were separated by ultrafiltration (MWCO 3000 Da, centrifugation at 4000 rpm for 10 min). The filter was re-washed twice with fresh PBS and centrifugated at the same condition. The MT-LIPs were harvested by refilling the filter with PBS and collecting the liquid manually. The ultrafiltrate in the collection tube, which contained the un-entrapped MT, was subjected to

colorimetric determination. The amount of the un-entrapped MT was quantified using a standard curve method, while LCs (loading capacity) and EEs (entrapment efficiency) were calculated as follows:

$$\mathrm{LC}(\%)\frac{\mathrm{W_{Total}}-\mathrm{W_{Free}}}{\mathrm{W_{Quality}}}*100\%$$

$$\mathrm{EE}(\%)\frac{\mathrm{W_{Total}}-\mathrm{W_{Free}}}{\mathrm{W_{Total}}}*100\%$$

Where W_{Total} is the total amount of MT feeded, W_{Free} is the amount of un-entrapped MT, and $W_{Quality}$ is the weight of MT-LIPs or TAT-MT-LIPs, respectively.

In vitro Release of MT from MT-LIPs and TAT-MT-LIPs

Dynamic membrane dialysis was employed to investigate the in vitro release profile of MT from liposomes using the method described previously,[44] with some modifications. Briefly, 2 mL of free MT, MT-LIP, or TAT-MT-LIP (all at the equaled MT concentration of 0.5 mg/mL) were transferred to a dialysis bag (MWCO 3500 Da) and immersed in 20 mL of PBS. The dialysis was performed at 37 °C in a rotating shaker with a speed of 100 rpm. At regular intervals, 2 mL of dialysate was replaced with 2 mL of fresh PBS. The amount of released MT was quantified by the above mentioned methods, and the cumulative release percentages were calculated.

In vitro and in vivo Toxicity Assessment

The cytotoxicity of MT-LIPs and TAT-MT-LIPs against HCECs was evaluated using a cell counting kit-8 assay (CCK-8, Dojindo Laboratories, Japan).[32] The HCECs were maintained in DMEM/F12 medium (Gibco, Waltham, MA, USA) supplemented with 10% fetal bovine serum (Gibco), 1% streptomycin-penicillin (PH1513, Phygene, USA) and 0.005 mg/mL insulin (Gibco). HCECs were seeded in 96-well plates at a density of 8×10^3 cells / 100 μL per well and incubated at 37 °C with an atmosphere of 5% CO_2 and 95% humidity. After treatments with varied amounts of free MT, MT-LIP, or TAT-MT-LIP for 24 or 48 h, the cells were co-cultured with a medium including 10% CCK-8 solution for 2 h under dark. The optical density (OD) at 450 nm was recorded by SpectraMax M5 plate reader (Molecular Devices, CA). To evaluate the safety of the formulas against eyes, we used the rats that were topically administrated with one drop (20 μL) of MT, MT-LIPs, 5% TAT-MT-LIPs, or 10% TAT-MT-LIPs (all at the equaled MT-concentration of 100 μM) at a time for once per day. Then, the corneas of rats were stained with sodium fluorescein and underwent medical examinations by a skilled doctor using a slit lamp at day 0, −4, −9, and −14 after topical administration. The intraocular pressure values were measured by a Schiotz tonometer (TV01, Icare, Finland) at the same time.

Cell Uptake Evaluation

To visualize the cell uptake behaviors of the liposomes with various modifications, we used the coumarin-6 fluorescence probe (C6) instead of MT was encapsulated into the liposomes. The liposomes were then co-cultured with HCECs in 24-well plates at a cell density of 3.5×10^5 cells / mL. After indicated treatments of 1, 3, 6, and 24 h, the cells were washed twice with 1 mL of HBSS, fixed with 4% paraformaldehyde for 10 min, and stained with DAPI. Fluorescent images were acquired using a confocal laser scanning microscope (CLSM, LSM880, Carl Zeiss Jena, Germany). To quantify the cell uptake behaviors, we obtained the cell suspensions after disassociation (0.25% trypsin for 3 min), centrifugation (1000 rpm, 4 min), and resuspension with PBS. The cell uptake behaviors on varied liposomes were then characterized by flow cytometry (BD C6 Plus).

Evaluation of the Retention of MT on the Eye Surface

Since multiple biological barriers exist on the eye surface, more than 90% of topically-administrated drugs are rapidly removed from the eye surface, which dramatically limits their therapeutic effects.[45] To understand the impacts of TAT on the retention of MT-LIPs in the cornea, the MT-LIPs (20 μL, MT-concentration of 100 μM) with varied amounts of TAT modifications were topically applied on SD rats, and the MT concentrations in the cornea were determined in a time-

dependent manner. The free MT in saline was also applied using the same method. During regular time intervals, the animals were sacrificed, and the corneas were obtained through a surgical process operated by a skilled doctor. The MT in the cornea was extracted with the following procedure: samples were completely ground in acetonitrile-ammonium acetate solution to release the MT. It was then extracted by ethyl acetate. The MT samples were obtained after nitrogen treatment to remove ethyl acetate and re-dissolve in acetonitrile. With appropriate dilution, the MT was quantitatively analyzed by UPLC-MS-MS (LC-8050, Shimada) equipped with a Shim-pack XR-ODS III chromatography column and a triple quadrupole mass spectrometer (MS). Specifically, the samples (2 μL) were auto-injected into the UPLC-MS-MS system and eluted with 0.1% formic acid in water (phase A) and methanol (phase B) at a speed of 0.4 mL/min with the following gradient process: 0–3 min, 10–90% B; 4.5 min, 90% B; 5 min, 10% B; and 7 min, 10% B. After column separation, the samples were detected by MS performed in Auto-MSn mode. The MS was conducted under the following conditions: ionizer, electrospray ionizer (ESI) performed under positive mode; capillary voltage, 4 kV; nebulizing gas flow, 3 L/min; drying gas flow, 10 L/min; heating gas flow, 10 L/min; the interface temperature, 350 °C; desolvation area temperature, 200 °C; and heart block temperature, 400 °C. The critical peak area of m/z 233.05>174.05 was employed for quantitative analysis.

To visualize the effect of TAT on the retention of LIPs, we used a cyanidin 3 (CY3) fluorescence probe instead of MT was loaded into the liposome (CY3-LIPs). Ten μL of the CY3-LIPs, 5%TAT- CY3-LIPs, and 10%TAT- CY3-LIPs were dropped into the conjunctival sac of rats every 10 min 3 times. After the last administration, the rats were sacrificed at 10-, 30-, 60-, and 90- min. The frozen sections of corneas were prepared and observed under CLSM.

Evaluation of Therapeutic Effects of MT Formula on DED

To develop BAC-DED, the animals were topical administered with 0.2% BAC twice daily for 14 consecutive days.[46] To understand the therapeutic effects of BAC-DED, different MT formulas (20 μL, containing 100 μM of MT) were topically treated once a day. The experiments were divided into five groups listed as follows: (I) rats treated with saline (healthy control); (II) rats treated with 0.2% BAC (in saline); (III) rats treated with 0.2% BAC+100 μM melatonin (in saline); (IV) rats treated with 0.2% BAC+MT-LIPs; (V) rats treated with 0.2% BAC+5% TAT-MT-LIPs; (VI) rats treated with 0.2% BAC + 10% TAT-MT-LIPs. On the 0th-, 4th-, 9th-, and 14th -days, the corneas were stained with 2% sodium fluorescein and evaluated under a slit lamp microscope.[33] The changes in intraocular pressure were traced using a Schiotz tonometer. The tear volume was monitored through a tear Schirmer test performed by a skilled doctor.

To further explore the therapeutic effects of MT formulas, the rats receiving various treatments were sacrificed after 14 days. The frozen sections of corneas with a thickness of 10 μm were prepared for immunofluorescence staining using the method described previously.[47,48] The sections were incubated with the primary antibodies at 4 °C overnight, followed by the corresponding secondary antibodies under room temperature for 2 h. The primary antibodies used in this study were listed as follows: mouse anti-DNA/RNA Damage (1:100, Abcam, RRID: ab62623); rabbit anti-NLRP3 (1:100, GeneTex, RRID: GTX00763); rabbit anti-IL-1 β (1:100, Protein tech, RRID: 26048-1-AP); rabbit anti-Caspase 1/p20/p10 (1:100, Protein tech, RRID: 22915-1-AP); rabbit anti-GSDMD (1:200, Protein tech, RRID: 20770-1-AP); the nuclei were stained with DAPI (P0131, Beyotime, Shanghai, China). The images were recorded by CLSM and quantified by ImageJ software.

Statistical Analysis

The data are expressed as means ± SDs. Statistical comparisons were performed using one-way ANOVA, and the $p < 0.05$, $p < 0.01$, and $p < 0.01$ were indications of statistical difference.

Results

Characterization of TAT-MT-LIPs and MT-LIPs

The TAT was chemically grafted onto the Mal-PEG_{2000}-DSPE by Michael's addition between the sulfhydryl group in TAT and the maleimide group in Mal-PEG_{2000}-DSPE (Figure 1). The product was identified by ^{1}H-NMR. After the reaction, the characteristic maleimide peak at chemical shift value (δ) of 6.72 ppm in Mal-PEG_{2000}-DSPE disappeared

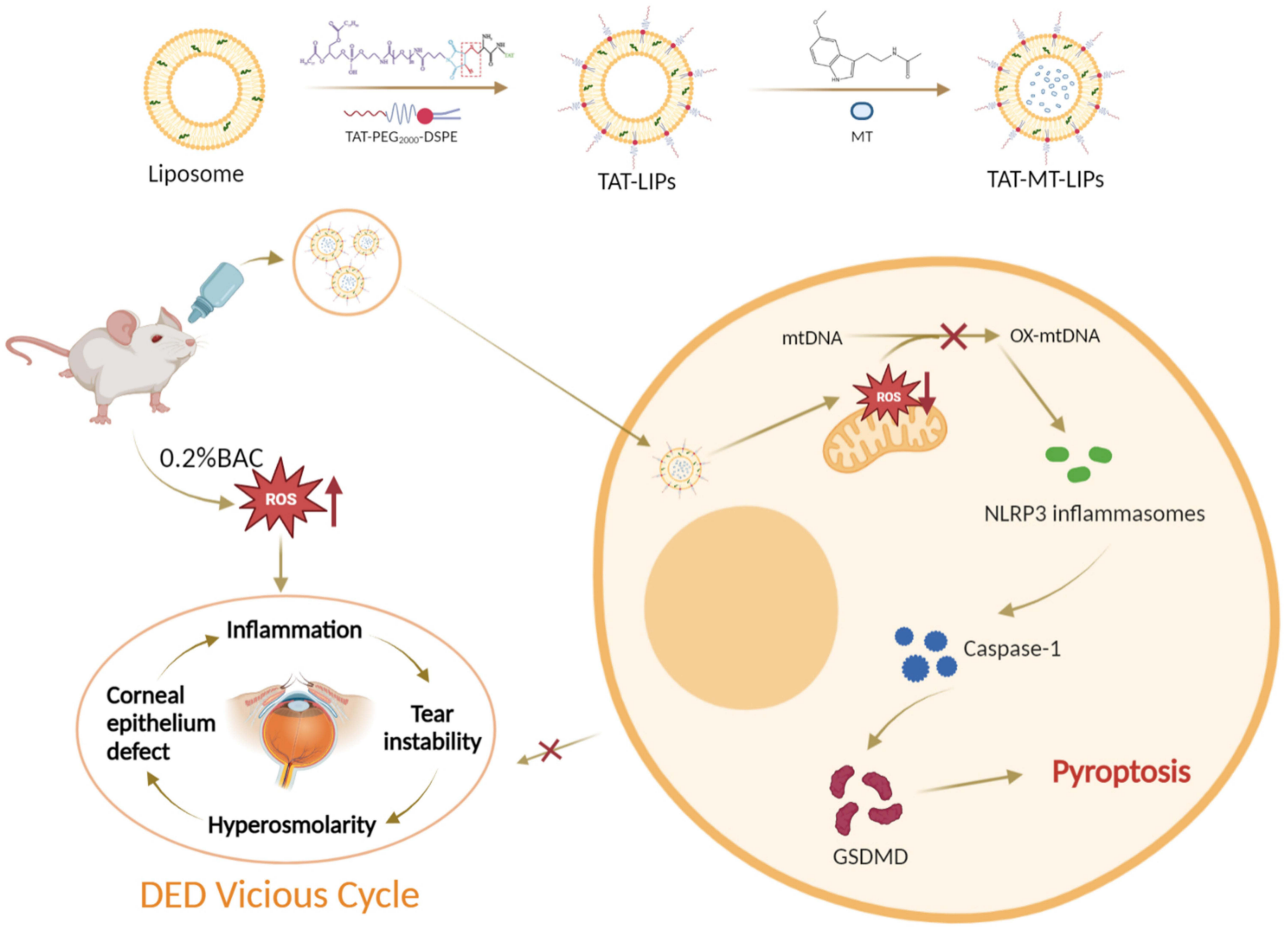

Figure 1 Schematic representation of preparation and application of TAT-MT-LIPs. The TAT was chemically grafted onto the Mal-PEG_{2000}-DSPE by Michael's addition between the sulfhydryl group in TAT and the maleimide group in Mal-PEG_{2000}-DSPE. TAT-MT-LIPs were prepared using film dispersion followed by the extrusion method and topically treated in rats once a day. Continuously ocular surface exposure of 0.2% BAC caused substantial mt-DNA oxidation, which promoted the transduction of NLRP3/Caspase-1/GSDMD and consequent corneal epithelium pyroptosis. TAT-MT-LIPs could break the "DED vicious cycle" by efficiently suppressing the BAC-induced corneal epithelium pyroptosis and inflammation by inhibiting mt-DNA oxidation and the subsequent signal transmission.

(Figure 2a), indicating the obtained TAT-modified PEG_{2000}-DSPE (TAT-PEG_{2000}-DSPE).[49] The size, dispersity, and zeta potential of the prepared liposomes were measured by DLS. Figures 2b and c show that the MT-loaded liposome formed by HSPL and cholesterol has a hydrodynamic size of around 200 nm (PDI: 0.1–0.2) and zeta potential around −50 to −55 mV. Increasing the proportion of cholesterol did not significantly affect the size, zeta potential, and PDI of liposomes. To obtain TAT grafted liposome, the HSPL was partly replaced by TAT-PEG_{2000}-DSPE at a designated amount for liposome preparation. As depicted in Figures 2d and e, the zeta potential increased from −57 mV to −16 mV, along with raising the ratio of TAT-PEG_{2000}-DSPE. However, the addition of TAT-PEG_{2000}-DSPE did not influence the size of the liposomes. The encapsulation ability of these liposomes for MT was evaluated. As shown in Figure 2f and g, 60–80% of the drug (corresponding to the loading capacity of 3–4%) were encapsulated into these liposomes when 0.5 mg of MT was fed, which were comparable to previously reported liposomes.[43] As expected, TAT modification did not change the encapsulation ability (Figure 2h) and release rate of the liposomes, which exhibited significantly lower than the free MT group; almost 90% of the drug was released within 3 h (Figure 2i). To verify whether the melatonin released form liposome carriers remains biologically active, we further test the free radical clearance ability of MT liposomes. As shown in Figure S1, the free radical clearance ability of MT liposomes was kept stable even after 30 h, indicating the effective biological activity of MT released from the liposome carriers. Meanwhile, the morphologies of the liposomes were observed by TEM. As depicted in Figure 2j, these MT-loaded liposomes displayed typically spherical nanostructure, which also remained after TAT modification.

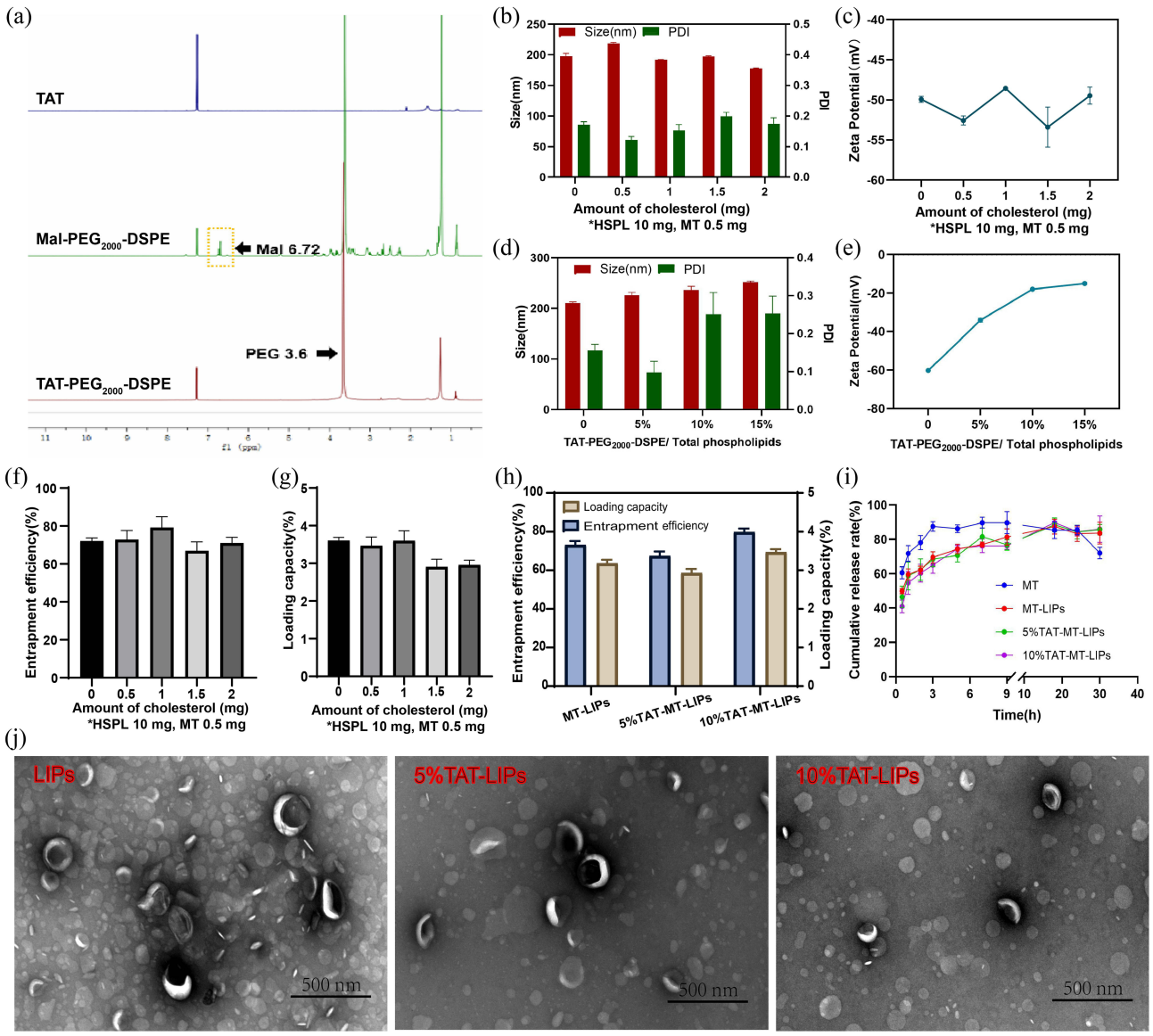

Figure 2 Preparation and characterization of the TAT-MT-LIPs. (**a**) ^{1}H-NMR spectra of TAT, Mal-PEG$_{2000}$-DSPE, and TAT-PEG$_{2000}$-DSPE. (**b** and **c**) The effect of cholesterol on the size, PDI, and zeta potential of liposomes. (**d** and **e**) The effect of TAT-PEG$_{2000}$-DSPE on the size, PDI, and zeta potential of liposomes. (**f** and **g**) The effect of cholesterol on the liposome's entrapment efficiency and loading capacity for MT. (**h**) The effect of TAT-PEG$_{2000}$-DSPE on the liposome's entrapment efficiency and loading capacity for MT. (**i**) the release profile of MT from liposomes. (**j**) The TEM images of the liposomes.

In vitro and in vivo Toxicity of the MT-LIPs

The CCK-8 assay was adopted to evaluate the cytotoxicity of MT and MT liposomes against HCECs. Excellent biocompatibility was detected in MT groups at a concentration range of 50–400 μM (Figure S2), and MT-LIPs, 5% TAT-MT-LIPs, and 10% TAT-MT-LIPs groups loaded MT with a concentration range of 25–100 μM after incubating for 24 h or 48 h (Figure 3a and b). The in vivo toxicity of MT, MT-LIPs, 5% TAT-MT-LIPs, and 10% TAT-MT-LIPs were evaluated by topically administrated once a day for continuous 14 days at a dose of 20 μL (MT concentration: 100 μM). As shown in Figure 3c, free MT elevated the IOP of rats up to 40% after 4 days, while it dropped to normal levels on the 9- and 14-days. While MT-LIPs, 5% TAT-MT-LIPs, and 10% TAT-MT-LIPs treatments did not significantly vibrate the IOP at the examined time point. Moreover, clinical examinations for corneas after topical administration of MT and MT liposomes were recorded by slit lamp under bright and cobalt blue light (Figure 3d and S3). All the treatments did not

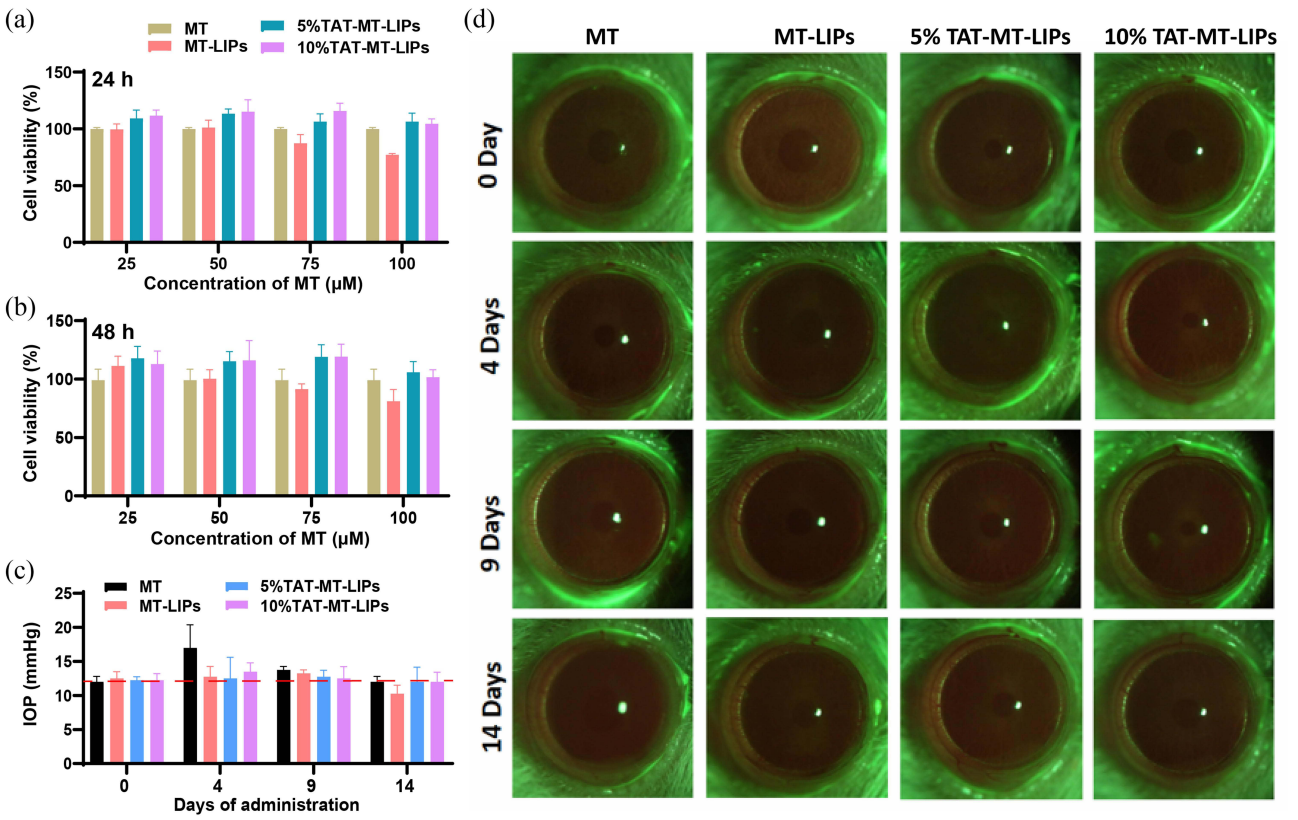

Figure 3 In vitro and in vivo toxicity of MT-LIPs. (**a** and **b**) The in vitro cytotoxicity of MT-LIPs. 5% TAT-MT-LIPs, and 10% TAT-MT-LIPs. (**c**) The effects of free MT, MT-LIPs. 5% TAT-MT-LIPs, and 10% TAT-MT-LIPs on the intraocular pressure (IOP) of healthy rats. Rats were treated with different MT formulas once a day. (**d**) Examination of the corneal lesions and defects with a slit lamp (magnification, 10×) under a cobalt blue light model. Rats were treated with different MT formulas once a day. Images were recorded after fluorescein staining.

cause significant pathological changes such as corneal edema, transparency, and other acute irritant reactions, suggesting that MT-LIPs and TAT-MT-LIPs can be safely applied to the eyes.

TAT-MT-LIPs Increase the Bioavailability of MT

To visualize the effects of TAT on cell uptake for liposomes, coumarin-6 (C6, fluorescence probe) instead of MT was encapsulated into the liposomes. After treatments of 1-, 3-, 6-, and 24-h, the cell uptake profiles of free C6, C6 in empty liposomes (C6-LIPs), C6 in 5% TAT-LIPs (5% TAT-C6-LIPs), and C6 in 10% TAT-LIPs (10% TAT-C6-LIPs) in HCECs were recorded by CLSM. As depicted in Figure 4a-d, the limited uptake ability of free C6 was slightly heightened by encapsulation into the liposomes while robustly enhanced by encapsulation into the TAT-modified liposomes. Meanwhile, the 10% TAT-C6-LIPs exhibited superior cell uptake than the 5% TAT-C6-LIPs. Interestingly, the amount of C6 increased by TAT-modified liposomes was primarily located in the cytoplasm where mitochondria rest, indicating the superiority of TAT-modified liposomes to encapsulate MT for mitochondria protection. The cell uptake was quantitatively analyzed by flow cytometry (Figures 4e and f), which further confirmed the observation on CLSM. These results suggested that encapsulation into TAT-modified liposomes could significantly improve the drug uptake by the corneal epithelial cells.

We further used rats to examine the effects of TAT modification on MT retention in corneas. After receiving the treatments of free MT, MT-LIPs, 5% TAT-MT-LIPs, and 10% TAT-MT-LIPs, the concentration of MT in the cornea was determined. As shown in Figures 5a and b, the concentration of MT rapidly dropped in 90 mins post-administration. The MT encapsulated into TAT-modified liposomes (5% TAT-MT-LIPs, and 10% TAT-MT-LIPs) significantly prolonged its retention in the cornea compared to free MT and MT in empty liposomes (MT-LIPs). To further understand the distribution of the liposomes, they were labeled with a CY3 fluorescence probe. After topical administration for

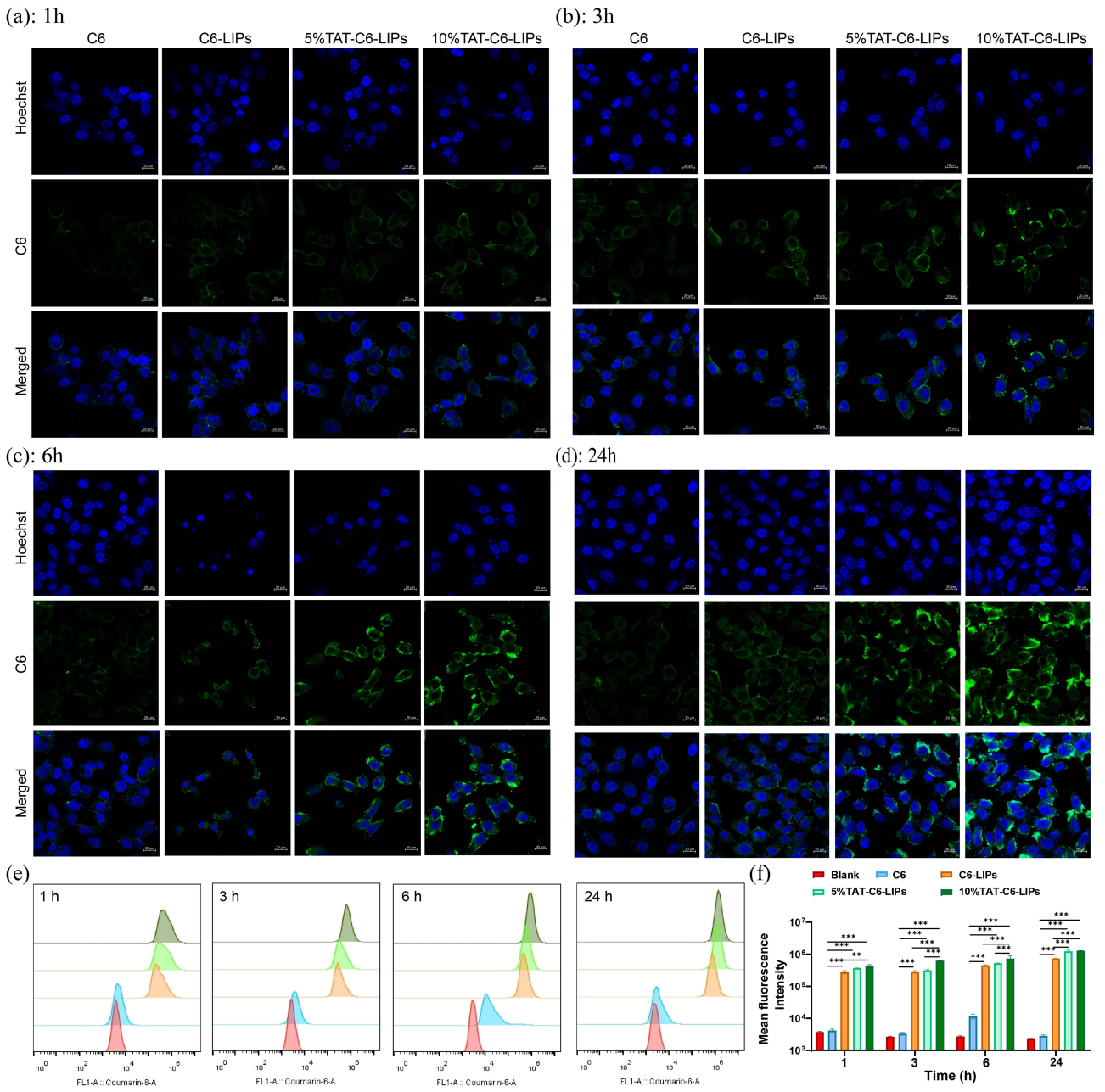

Figure 4 The effects of TAT modification on cellular (HCECs) uptake behaviors. (**a-d**) CLSM observation of cellular (HCECs) liposome uptake with or without TAT modification. Scale bar=20 μm. (**e**) Flow cytometry evaluation of cellular (HCECs) uptake, and (**f**) quantification of cellular (HCECs) uptake. ** p<0.01, *** p<0.001.

a certain time, the frozen sections of corneas were prepared and then observed by confocal microscopy. As shown in Figure 5c, the cornea treated with 5% TAT-CY3-LIPs and 10% TAT-CY3-LIPs exhibited obviously higher CY3 signals than the free CY3 and CY3-LIPs treatments 60 mins after administration, which are consistent with the phenomenon observed in Figure 4a. Notably, the drug was mainly distributed in the epithelium of the cornea, which may benefit DED therapy as the DED was characterized by the abnormal corneal epithelium.[50]

TAT-MT-LIPs Alleviate the Clinical Symptoms of BAC-DED

After receiving various treatments, the experimental animals were medically examined for typical clinical symptoms of BAC-DED under a slit-lamp (Figures 6a, b, S4 and S5). As shown in Figure 6b, the cornea exhibited a large area of agglomerate fluorescence staining after BAC-DED modeling for 4 days, indicating a defect of corneal epithelium. The MT exerted apparent

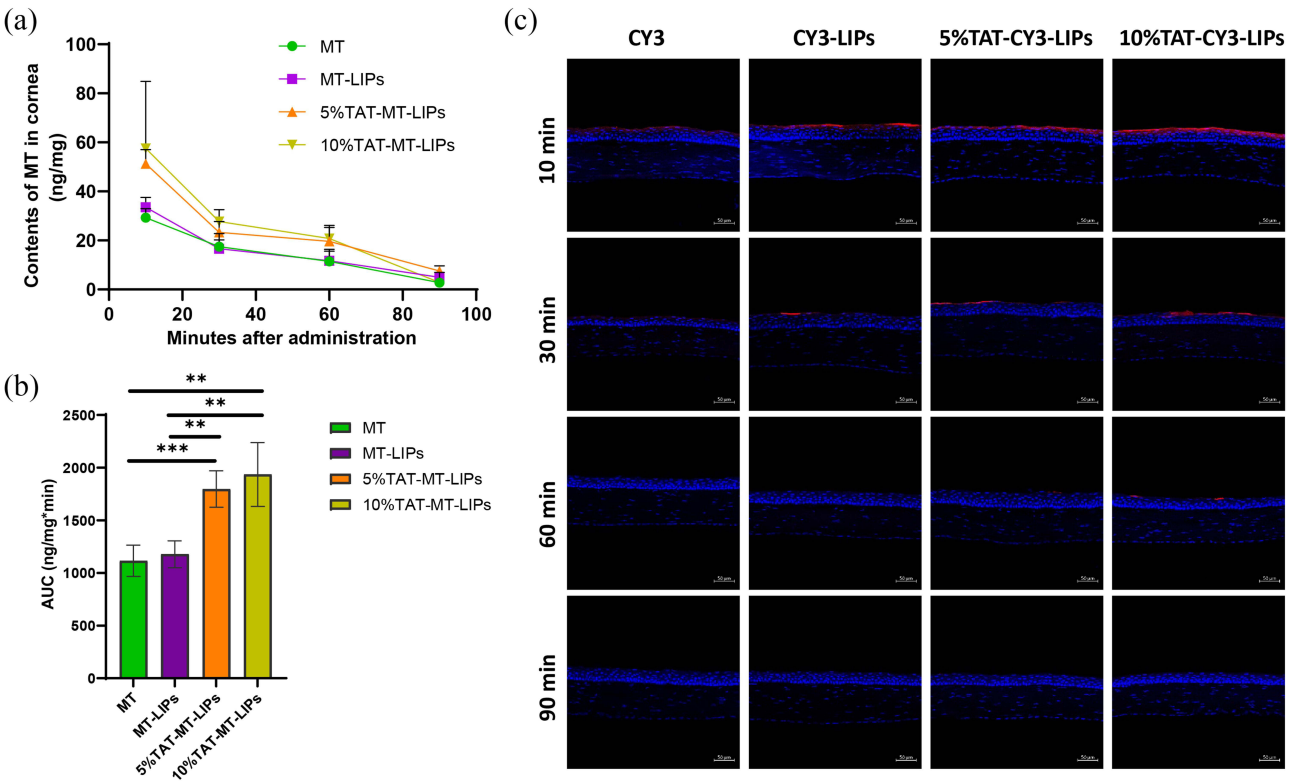

Figure 5 The effects of TAT modification on the retention of drugs in the cornea. (**a**) The changes of MT contents in the cornea, and (**b**) the calculated area under the curve (AUCs). ** p<0.01, *** p<0.001. (**c**) CY3 probe indicates the time-dependent distribution of the liposomes in the cornea. Scale bar=50 μm.

protective effects on corneal epithelium; thus, reduced staining area could be observed in the cornea receiving free MT treatment with dose-dependent property (Figures 6b, c, s4b, s4d and s4g). Encapsulation of MT into TAT-modified liposomes enhanced its beneficial effects on combating BAC-induced corneal epithelium defect that negligible fluorescence staining could be observed when treated with 5% TAT-MT-LIPs or 10% TAT-MT-LIPs (Figures 6b and c). Meanwhile, continuously dropping 0.2% BAC solution (twice a day) could cause persistent ocular surface inflammation and corneal edema (Figures 6d, e and s4a). Topical treatments with free MT or MT-LIPs could significantly reduce ocular surface inflammation and corneal edema compared to the normal saline treatment (Figures 6d, e and S5). However, there still exhibited markedly higher than the healthy control. After applying 5% TAT-MT-LIPs and 10% TAT-MT-LIPs, the corneal edema and ocular surface inflammation levels were dropped to healthy control (no significant difference with the healthy group). Otherwise, the intraocular pressure of rats was followed during the experimental time range. As depicted in Figure 6f, the healthy rats sustained intraocular pressure of 9–12 mmHg. Topical administration of 0.2% BAC significantly elevated the intraocular pressure to 14.4 ± 1.7 mmHg, 18.4 ± 2.7 mmHg, and 15.6 ± 1.1 mmHg at the 4th-, 9th-, and 14th-days after drug administration, respectively (Figure 6f). Free MT could lower the intraocular pressure while still significantly higher than healthy control. The TAT-MT-LIPs exhibited superior in preventing the BAC-induced intraocular pressure than free MT and MT-LIPs (without TAT). Moreover, TAT-MT-LIPs presented more efficiency in restoring tear secretions under BAC-DED (Figure S6). These results suggested that TAT-MT-LIPs exerted more potential than free MT and bare MT-LIPs to inhibit BAC-induced DED.

TAT-MT-LIPs Prevent Conjunctival Goblet Cells Loss in BAC-DED

The loss of conjunctival goblet cells that secrete mucin to maintain the stability of tear film is the typical consequence of DED.[51] The periodic acid Schiff (PAS) staining was conducted to evaluate the effects of these MT formulas on conjunctival goblet cells under BAC-DED. As shown in Figure S7, the number of conjunctival goblet cells dropped markedly after BAC instilling. The conjunctival goblet cell counts were significantly higher with the treatments of various MT formulas compared to the treatment of normal saline, suggesting the protective effects of MT against BAC-

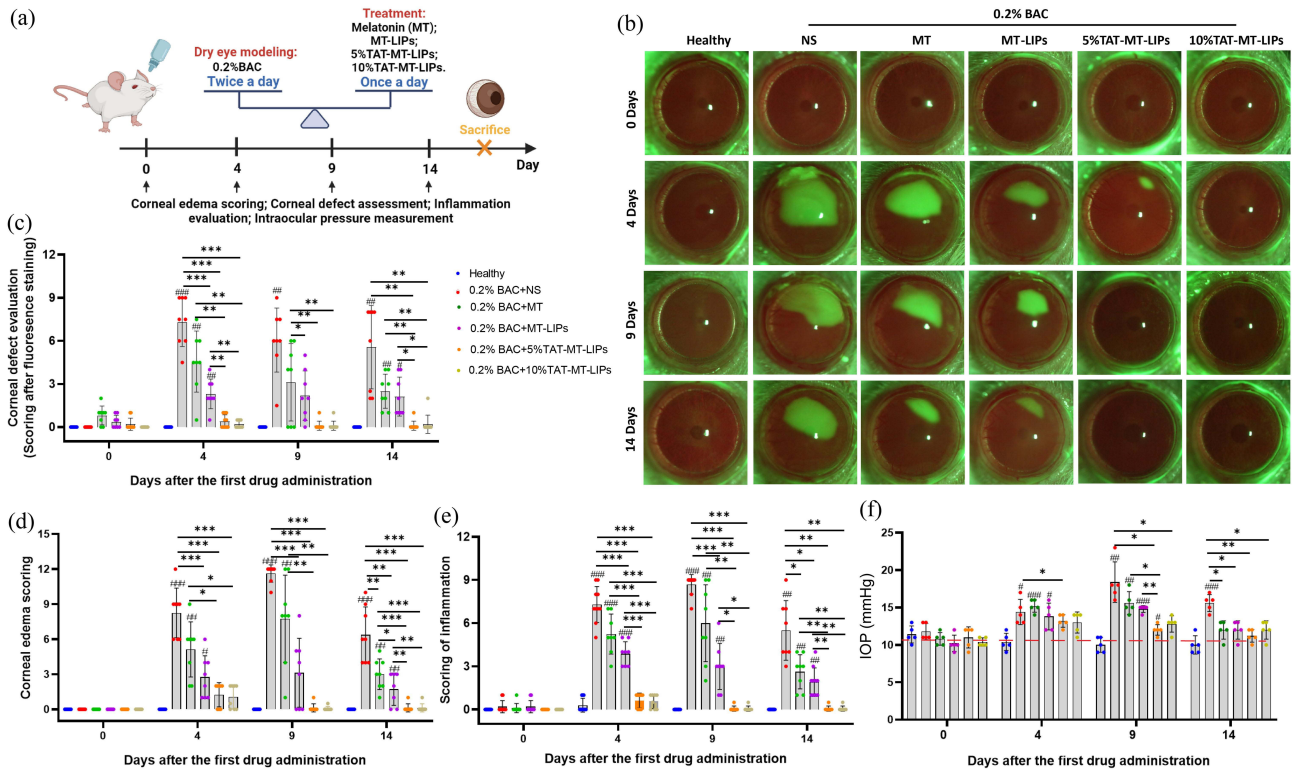

Figure 6 TAT-MT-LIPs alleviate clinical DED symptoms of the BAC-treated rats. (**a**) Schematic representation of the application of TAT-MT-LIPs. (**b**) Examination of corneal lesions and defects by slit lamp (magnification, 10×) under cobalt blue light model. (**c-e**) Evaluation (scoring) of corneal defect, -edema, and -inflammation. (**f**) Changes of IOP after receiving various treatments. Data are mean ± SD. Significance was assessed using one-way ANOVA. *p<0.05, **p<0.01, ***p<0.001; # p<0.05, ## p<0.01, ### p<0.001 Compares to the healthy control.

induced toxicity. Among these MT formulas, TAT-MT-LIPs exerted more effectiveness in increasing the number of goblet cells than free MT and bare MT-LIPs, demonstrating the superiority of TAT application in ocular surface disease therapy.

TAT-MT-LIPs Inhibit Mitochondrial DNA Oxidation

MT is preferably distributed in mitochondria as an effective mitochondrial ROS scavenger.[20–22] To further understand the beneficial effects of these MT formulas, cornea-sections from the animals receiving various treatments were prepared and subjected to immunofluorescence staining of 8-hydroxydeoxyguanosine (8-OHdG, products of DNA oxidation), which is generally regarded as a biomarker for intraocular oxidative stress.[52] As depicted in Figures 7a and b, BAC caused substantially oxidative DNA damage. Noticeably, most of the 8-OHdG fluorescence signals were nonoverlapped with the DAPI (Figure 7c and d), indicating mitochondrial DNA is the major DNA hit of the oxidative condition under DED. All these MT formulas can significantly reduce mitochondrial DNA oxidation after BAC-DED modeling (Figure 7a and b), suggesting MT can serve as a mitochondrial-targeted antioxidant in eye surface medication. Moreover, the encapsulation of MT into liposomes significantly enhanced its capacity to inhibit mitochondrial DNA oxidation. Among them, 10% TAT-MT-LIPs treatment displayed nearly un-detectable 8-OHdG staining close to the healthy group, demonstrating its best effects in inhibiting mitochondrial DNA oxidation (Figure 7a and b).

TAT-MT-LIPs Suppress NLRP3/Caspase-1/GSDMD Signaling Transduction

ROS has been widely investigated to be involved in the pathogenesis of DED by promoting the expression of NLRP3.[9,53,54] We have previously demonstrated that scavenging of mitochondrial ROS by antioxidative MitoQ/HA nanoparticles could inhibit environment-induced DED by down-regulation of NLRP3 expression.[33] In the present study, the effects of MT formulas on the changes of NLRP3/Caspase-1/GSDMD signaling axis, which consequent as pyroptotic cell death,[55,56] was

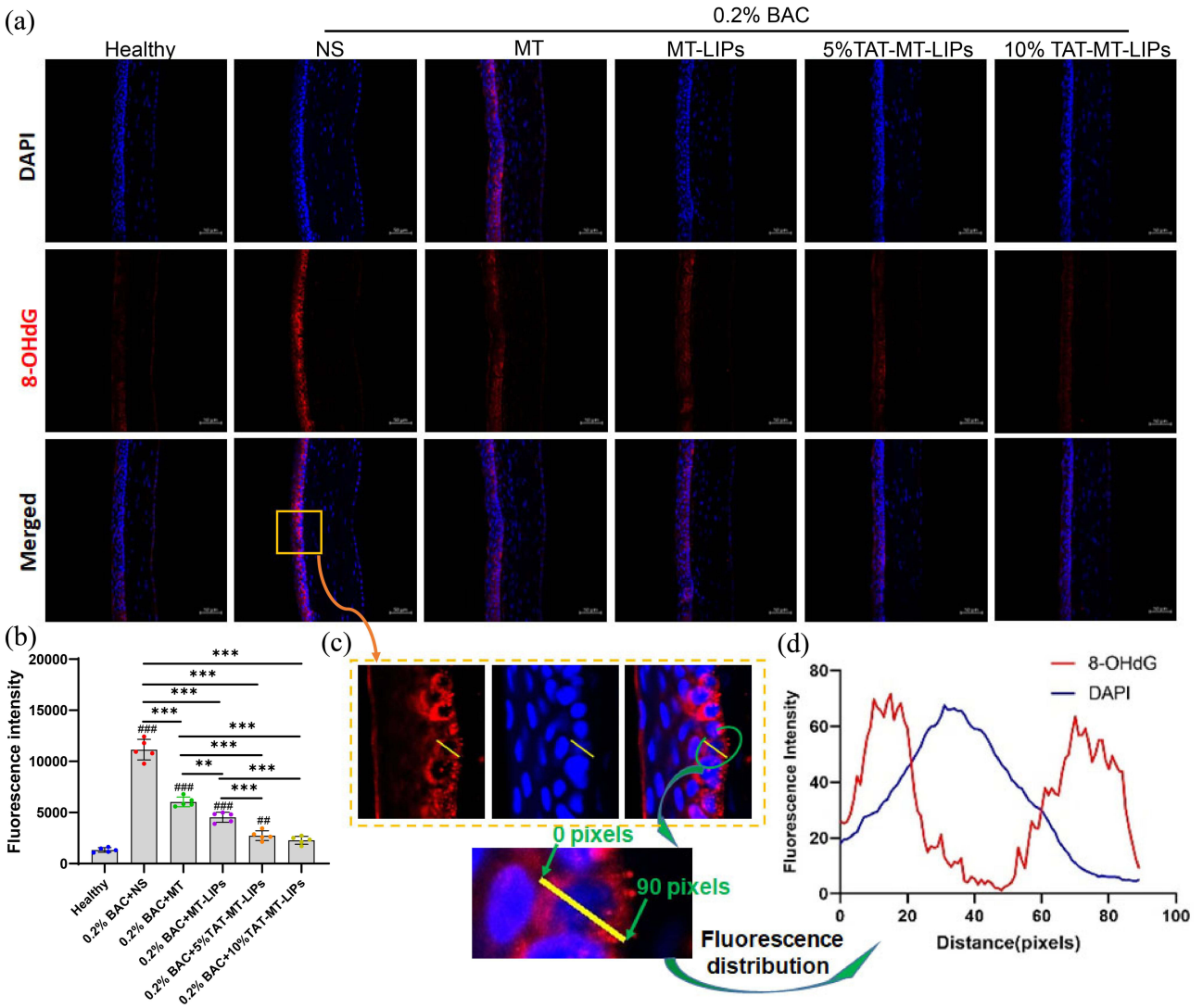

Figure 7 The effects of TAT-MT-LIPs on mitochondrial DNA (mt-DNA) oxidation. (**a**) 8-OHdG immunofluorescence staining. (**b**) Quantitative analysis of mt-DNA oxidation level. Data are mean ± SD. Significance was assessed using one-way ANOVA. ** p<0.01, *** p<0.001; ## p<0.01, ### p<0.001 Compares to the healthy control. (**c**) Enlarged images to map the 8-OHdG (DNA oxide). (**d**) The fluorescence intensity distribution of DAPI and 8-OHdG.

investigated by fluorescence immune-staining (Figures 8a-d). As depicted, the BAC sharply up-regulated the expression of NLRP3, Caspase-1, GSDMD, as well as the IL-1β by 6.2-, 5.9-, 8.8-, and 10.3-fold, respectively, when compared to the healthy control (Figures 8e-h). Compared to normal saline treatment, free MT treatment could significantly down-regulate the expression of NLRP3, Caspase-1, GSDMD, as well as IL-1β by 22%, 31%, 42%, and 26%, respectively (Figures 8e-h). However, there were still significantly higher than the healthy control. Encapsulation of MT into TAT-modified liposomes showed the best capacity among all the liposomes in suppressing NLRP3/Caspase-1/GSDMD transduction and IL-1β secretion, indicating the robust power in inhibition of NLRP3 inflammasome that resulting attenuation of pyroptosis and inflammatory at the meantime, which was further confirmed by evidences in vitro (HCECs) (Figures S8). These results demonstrated that TAT-MT-LIPs could be an excellent choice as the medicament against BAC-DED.

Discussion

BAC, a quaternary ammonium compound, is widely employed as an antimicrobial preservative in eye drops and hard contact lenses.[1] Eye-drops represent the most prescribed formulas in clinical ophthalmology,[57] which evoke attention to its side effects. BAC can disrupt the lipid and denature the proteins in cytoplasmic membranes.[2,3] Continues exposure to

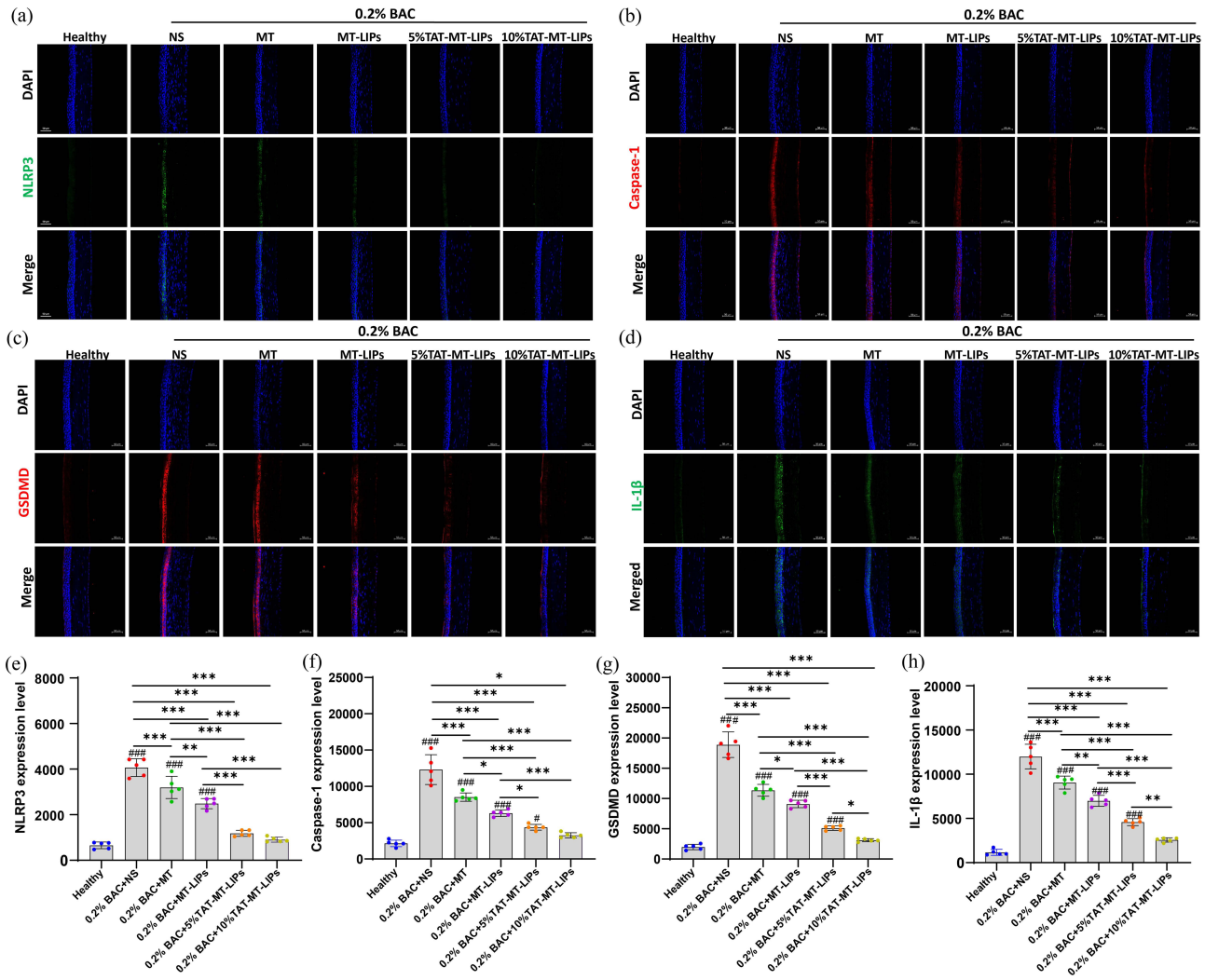

Figure 8 Histological analysis of the corneas. (**a-d**), Representative images of NLRP3, Caspase-1, GSDMD, and IL-1β immunofluorescence staining. (**e-h**), Quantitative analysis of expression level of NLRP3, Caspase-1, GSDMD, and IL-1β. Data are mean ± SD. Significance was assessed using one-way ANOVA. *p<0.05, **p<0.01, ***p<0.001; #p<0.05, ###p<0.001 Compares to the healthy control.

BAC induces a large of chronic DED-alike changes in ocular surface tissues (eg, corneal epithelium defect, conjunctival goblet cell loss, tear film instability, and persistence ocular surface inflammation),[2–4] by which is generally employed to establish the classical animal model of DED.[46] Previous studies suggested repeated exposure to BAC induced the apoptosis of conjunctival cells,[58] corneal epithelial cells,[59] and lung epithelial cells.[60] However, the mechanism underlying how the topical BAC induces DED-alike changes in an ocular surface is still largely unclear. Since the NLRP3 has been intensively reported to be involved in the pathogenesis of DED,[54] we evaluated the changes of NLRP3/Caspase-1/GSDMD pyroptosis cascade in the cornea of a rat receiving BAC topical treatment. Results showed that BAC caused substantial corneal epithelium loss while significantly up-regulated the expression of NLRP3, Caspase-1, and GSDMD, suggesting pyroptosis may be involved in corneal epithelium loss under BAC-DED. Since chloride can regulate NLRP3-dependent inflammation signal transduction,[61] this side effects of BAC (promoting pyroptotic corneal epithelium death) could be a result of the ionic chlorine in BAC. However, further efforts are needed to clarify this point.

The transduction of the NLRP3/Caspase-1/GSDMD signaling axis relies on the activation of the NLRP3 inflammasome, which is a multi-molecular platform with a sensor (NLRP3), an adaptor (ASC) and an effector (Caspase-1) assembled with the regulation of various micro-environmental triggers.[10,11] Under DED, ROS triggered the overexpression of NLRP3.[9,53] However, how does the ROS affect the formation of the NLRP3 inflammasome, thereby promotes the

transduction of NLRP3/Caspase-1/GSDMD signaling axis is still largely blurred. ROS can attack the mitochondrial-DNA (mt-DNA), -lipids, and -protein, thus causing the mitochondria to lose structural/functional integrity. Li et al have demonstrated that cytosolic release of oxide mitochondria DNA (ox-mt-DNA) directly binds to NLRP3 protein that triggers the activation of NLRP3 inflammasome.[62] In this study, we have observed that BAC significantly boosted the mt-DNA oxidation. While efficiency suppression of mt-DNA oxidation by TAT-MT-LIPs (MT are the mitochondria-specific antioxidant) can dramatically reduce mt-DNA oxidation concurrently down-regulate NLRP3, Caspase-1, GSDMD, and IL-1β. Though there is still some distance from perfect, preliminarily, we have concluded that oxidation of mt-DNA accumulated by ROS under BAC-DED can release cytosol out from mitochondria following activating the NLRP3 inflammasome. That may be a deep underlying mechanism for the promoted transduction of NLRP3/Caspase-1/GSDMD signaling axis, which consequent a pyroptotic death of corneal epithelium in BAC-DED. Though several reports have indicated the role of pyroptosis in the development of DED,[14,63,64] the BAC-induced corneal epithelium pyroptosis has not been reported before. The present study provided new insights into the adverse effects of BAC, which can serve as a new target for the protection of corneal epithelium when applying BAC as a preservative in eye drops.

As BAC induces substantial oxidation of mt-DNA, which promotes transduction of NLRP3/Caspase-1/GSDMD signaling axis, mitochondria-specific delivery of antioxidants for in situ scavenging of mitochondria ROS, thus inhibition of mt-DNA oxidation could block the pyroptotic NLRP3/Caspase-1/GSDMD signal transduction. MT is a mitochondrial target antioxidant that exerts its antioxidant activity by directly scavenging ROS and regulating the bioactivity of oxidation-reduction-related enzymes.[18,20–22] Our data showed that topical administration of MT could significantly reduce the BAC-induced mt-DNA oxidation, and suppress the expression of NLRP3, Caspase-1, GSDMD, as well as IL-1β at the meantime, nevertheless still higher than the level in health control. Considering the anatomical and physiological barriers that exist in the ocular surface that limit the bioavailability of applied agents,[30–32,65–68] we further encapsulated MT into TAT-modified liposomes, which prolonged the retention of MT in the cornea to enhance the cornea-epithelium-uptake for MT. With topical administration, TAT-MT-LIPs efficiently inhibited mt-DNA oxidation and, in sequence, suppressed the transduction of NLRP3/Caspase-1/GSDMD signaling axis and IL-1β secretion preventing the pyroptosis and inflammation of cornea epithelium under BAC-DED. By efficiently delivering MT, TAT-MT-LIPs significantly alleviated the DED-clinical symptom nearly to a healthy level, suggesting its potential to be developed as a new DED treatment.

Conclusion

The present study developed TAT-modified liposomes to efficiently deliver MT for inhibiting BAC-induced DED. After topical administration, TAT-MT-LIPs significantly alleviated DED-clinical symptoms of experimental animals by inhibiting tissue inflammation and preventing the loss of the corneal epithelium and conjunctival goblet cells. Our data suggested continuous ocular surface exposure of BAC-induced NLRP3/Caspase-1/GSDMD mediated corneal epithelium pyroptosis, which was not reported before. BAC caused substantial mt-DNA oxidation, which promoted the transduction of NLRP3/Caspase-1/GSDMD and consequent corneal epithelium pyroptosis. TAT-MT-LIPs could efficiently suppress the BAC-induced corneal epithelium pyroptosis and inflammation by inhibiting mt-DNA oxidation and the subsequent signal transmission. These results suggested the potential of TAT-MT-LIPs to be developed as a new DED treatment. Since BAC is widely employed as a preservative in eye drops, the present study provided new insights into the adverse effects of BAC, which can benefit for rational application of BAC as a preservative in eye drops.

Acknowledgments

This work was financially supported by the Basic Research Project of Wenzhou City (ZY2021018, Y20210195), Zhejiang Provincial Natural Science Foundation of China (LY19H120002, LQ23H120002), and the Innovation Promoting Project of Wenzhou Medical University Affiliated Eye Hospital (YNZD2201901, J02-20190202).

Disclosure

The authors report no conflicts of interest in this work.

References

1. Merchel Piovesan Pereira B, Tagkopoulos I. Benzalkonium chlorides: Uses, regulatory status, and microbial resistance. *Appl Environ Microbiol*. 2019;85:e00377–19.
2. Ittoop SM, Seibold LK, Kahook MY. Ocular surface disease and the role of preservatives in glaucoma medications. In: Shaarawy TM, Sherwood MB, Hitchings RA, Crowston JG, editors. *Glaucoma*. 2nd ed. Philadelphia, PA: Elsevier, Saunders WB; 2015:593–597.
3. Goldstein MH, Silva FQ, Blender N, Tran T, Vantipalli S. Ocular benzalkonium chloride exposure: Problems and solutions. *Eye*. 2022;36:361–368.
4. Zhang R, Park M, Richardson A, et al. Dose-dependent benzalkonium chloride toxicity imparts ocular surface epithelial changes with features of dry eye disease. *Ocul Surf*. 2020;18:158–169.
5. Schaumberg DA, Sullivan DA, Dana MR. Epidemiology of dry eye syndrome. *Adv Exp Med Biol Biol*. 2002;506:989–998.
6. Stapleton F, Alves M, Bunya VY, et al. TFOS DEWS II epidemiology report. *Ocul Surf*. 2017;15:334–365.
7. Tsubota K, Yokoi N, Shimazaki J, et al. New perspectives on dry eye definition and diagnosis: A consensus report by the Asia dry eye society. *Ocul Surf*. 2017;15:65–76.
8. Li S, Lu Z, Huang Y, et al. Anti-oxidative and anti-Inflammatory micelles: Break the dry eye vicious cycle. *Adv Sci*. 2022;9:e2200435.
9. Zheng Q, Ren Y, Reinach PS, et al. Reactive oxygen species activated NLRP3 inflammasomes prime environment-induced murine dry eye. *Exp Eye Res*. 2014;125:1–8.
10. Swanson KV, Deng M, Ting JPY. The NLRP3 inflammasome: molecular activation and regulation to therapeutics. *Nat Rev Immunol*. 2019;19:477–489.
11. Paik S, Kim JK, Silwal P, Sasakawa C, Jo EK. An update on the regulatory mechanisms of NLRP3 inflammasome activation. *Cell Mol Immunol*. 2021;18:1141–1160.
12. Tang TT, Lang XT, Xu CF, et al. CLICs-dependent chloride efflux is an essential and proximal upstream event for NLRP3 inflammasome activation. *Nat Commun*. 2017;8:202.
13. Domingo-Fernandez R, Coll RC, Kearney J, Breit S, O'Neill LAJ. The intracellular chloride channel proteins CLIC1 and CLIC4 induce IL-1 beta transcription and activate the NLRP3 inflammasome. *J Biol Chem*. 2017;292:12077–12087.
14. Zhang J, Dai Y, Yang Y, Xu J. Calcitriol alleviates hyperosmotic stress-induced corneal epithelial cell damage via inhibiting the NLRP3-ASC-Caspase-1-GSDMD pyroptosis pathway in dry eye disease. *J Inflamm Res*. 2021;14:2955–2962.
15. Evavold CL, Hafner-Bratkovic I, Devant P, et al. Control of gasdermin D oligomerization and pyroptosis by the Ragulator-Rag-mTORC1 pathway. *Cell*. 2021;184:4495–4511 e19.
16. Kayagaki N, Stowe IB, Lee BL, et al. Caspase-11 cleaves gasdermin D for non-canonical inflammasome signalling. *Nature*. 2015;526:666–671.
17. Tsai TY, Chen TC, Wang IJ, et al. The effect of resveratrol on protecting corneal epithelial cells from cytotoxicity caused by moxifloxacin and benzalkonium chloride. Invest. Ophth. *Vis Sci*. 2015;56:1575–1584.
18. Reiter RJ, Mayo JC, Tan DX, Sainz RM, Alatorre-Jimenez M, Qin L. Melatonin as an antioxidant: Under promises but over delivers. *J Pineal Res*. 2016;61:253–278.
19. Manchester LC, Coto-Montes A, Boga JA, et al. Melatonin: An ancient molecule that makes oxygen metabolically tolerable. *J Pineal Res*. 2015;59:403–419.
20. Reiter RJ, Tan D, Mayo JC, Sainz RM, Leon J, Czarnocki Z. Melatonin as an antioxidant: Biochemical mechanisms and pathophysiological implications in humans. *Acta Biochim Pol*. 2003;50:1129–1146.
21. Reiter RJ, Rosales-Corral S, Tan DX, Jou MJ, Galano A, Xu B. Melatonin as a mitochondria-targeted antioxidant: One of evolution's best ideas. *Cell Mol Life Sci*. 2017;74:3863–3881.
22. Jou MJ, Peng TI, Reiter RJ, Jou SB, Wu HY, Wen ST. Visualization of the antioxidative effects of melatonin at the mitochondrial level during oxidative stress-induced apoptosis of rat brain astrocytes. *J Pineal Res*. 2004;37:55–70.
23. Rastmanesh R. Potential of melatonin to treat or prevent age-related macular degeneration through stimulation of telomerase activity. *Med Hypotheses*. 2011;76:79–85.
24. Blasiak J, Reiter RJ, Kaarniranta K. Melatonin in retinal physiology and pathology: The case of age-related macular degeneration. *Oxid Med Cell Longev*. 2016;2016:6819736.
25. Wang B, Zuo X, Peng L, et al. Melatonin ameliorates oxidative stress-mediated injuries through induction of HO-1 and restores autophagic flux in dry eye. *Exp Eye Res*. 2021;205:108491.
26. Jin K, Ge Y, Ye Z, et al. Anti-oxidative and mucin-compensating dual-functional nano eye drops for synergistic treatment of dry eye disease. *Appl Mater Today*. 2022;27:101411.
27. Ashrafizadeh M, Najafi M, Kavyiani N, Mohammadinejad R, Farkhondeh T, Samarghandian S. Anti-inflammatory activity of melatonin: a focus on the role of NLRP3 inflammasome. *Inflammation*. 2021;44:1207–1222.
28. Che H, Li H, Li Y, et al. Melatonin exerts neuroprotective effects by inhibiting neuronal pyroptosis and autophagy in STZ-induced diabetic mice. *FASEB J*. 2020;34:14042–14054.
29. Liu QJ, Su LY, Sun CL, et al. Melatonin alleviates morphine analgesic tolerance in mice by decreasing NLRP3 inflammasome activation. *Redox Biol*. 2020;34:101560.
30. Rowe-Rendleman CL, Durazo SA, Kompella UB, et al. Drug and gene delivery to the back of the eye: from bench to bedside. *Invest Ophthalmol Vis Sci*. 2014;55:2714–2730.
31. Park CG, Kim YK, Kim MJ, et al. Mucoadhesive microparticles with a nanostructured surface for enhanced bioavailability of glaucoma drug. *J Control Release*. 2015;220:180–188.
32. Lin S, Ge C, Wang D, et al. Overcoming the anatomical and physiological barriers in topical eye surface medication using a peptide-decorated polymeric micelle. *ACS Appl Mater Interf*. 2019;11:39603–39612.
33. Zheng Q, Li L, Liu M, et al. In situ scavenging of mitochondrial ROS by antioxidative MitoQ/hyaluronic acid nanoparticles for environment-induced dry eye disease therapy. *Chem Eng J*. 2020;398:125621.
34. Nguyen D, Lai J. Synthesis, bioactive properties, and biomedical applications of intrinsically therapeutic nanoparticles for disease treatment. *Chem Eng J*. 2022;435:134970.

35. Assanhou A, Li W, Zhang L, et al. Reversal of multidrug resistance by co-delivery of paclitaxel and lonidamine using a TPGS and hyaluronic acid dual functionalized liposome for cancer treatment. *Biomaterials*. 2015;73:284–295.
36. Sang R, Stratton B, Engel A, Deng W. Liposome technologies towards colorectal cancer therapeutics. *Acta Biomater*. 2021;127:24–40.
37. Janagam DR, Wu L, Lowe TL. Nanoparticles for drug delivery to the anterior segment of the eye. *Adv Drug Deliv Rev*. 2017;122:31–64.
38. Zhang P. Monteiro da Silva G, Deatherage C, Burd C, DiMaio D. Cell-penetrating peptide mediates intracellular membrane passage of human papillomavirus L2 protein to trigger retrograde trafficking. *Cell*. 2018;174:1465–1476 e13.
39. Zou L, Peng Q, Wang P, Zhou B. Progress in research and application of HIV-1 TAT-derived cell-penetrating peptide. *J Membr Biol*. 2017;250::115–122.
40. Nguyen D, Luo L, Yang C, Lai J. Highly retina-permeating and long-acting resveratrol/metformin nanotherapeutics for enhanced treatment of macular degeneration. *ACS Nano*. 2023;17:168–183.
41. Yadavar-Nikravesh M-S, Ahmadi S, Milani A, et al. Construction and characterization of a novel Tenofovir-loaded PEGylated niosome conjugated with TAT peptide for evaluation of its cytotoxicity and anti-HIV effects. *Adv Powder Technol*. 2021;32:3161–3173.
42. Zhang H. Thin-film hydration followed by extrusion method for liposome preparation. *Methods Mol Biol*. 2017;1522:17–22.
43. Jose J, Kanniyappan H, Muthuvijayan V. A novel, rapid and cost-effective method for separating drug-loaded liposomes prepared from egg yolk phospholipids. *Process Biochem*. 2022;115:80–91.
44. Yi H, Lu W, Liu F, et al. ROS-responsive liposomes with NIR light-triggered doxorubicin release for combinatorial therapy of breast cancer. *J Nanobiotechnol*. 2021;19:134.
45. Agarwal P, Huang D, Thakur SS, Rupenthal ID. Nanotechnology for ocular drug delivery. In: Grumezescu AM, editor. *Design of Nanostructures for Versatile Therapeutic Applications*. 2018:137–188.
46. Lin Z, Liu X, Zhou T, et al. A mouse dry eye model induced by topical administration of benzalkonium chloride. *Mol Vis*. 2011;17:257–264.
47. Lin S, Gao W, Zhu C, et al. Efficiently suppress of ferroptosis using deferoxamine nanoparticles as a new method for retinal ganglion cell protection after traumatic optic neuropathy. *Biomater Adv*. 2022;138:212936.
48. Huang B, Li X, Tu X, et al. OTX1 regulates cell cycle progression of neural progenitors in the developing cerebral cortex. *J Biol Chem*. 2018;293:2137–2148.
49. Wu B, Li M, Li K, et al. Cell penetrating peptide TAT-functionalized liposomes for efficient ophthalmic delivery of flurbiprofen: penetration and its underlying mechanism, retention, anti-inflammation and biocompatibility. *Int J Pharm*. 2021;598:120405.
50. Yu C, Chen P, Xu J, et al. Corneal epithelium-derived netrin-1 alleviates dry eye disease via regulating dendritic cell activation. *Invest Ophthalmol Vis Sci*. 2022;63:1.
51. Swamynathan SK, Wells A. Conjunctival goblet cells: Ocular surface functions, disorders that affect them, and the potential for their regeneration. *Ocul Surf*. 2020;18:19–26.
52. Ock CY, Kim EH, Choi DJ, Lee HJ, Hahm KB, Chung MH. 8-Hydroxydeoxyguanosine: not mere biomarker for oxidative stress, but remedy for oxidative stress-implicated gastrointestinal diseases. *World J Gastroenterol*. 2012;18:302–308.
53. Zheng Q, Ren Y, Reinach PS, et al. Chen, Reactive oxygen species activated NLRP3 inflammasomes initiate inflammation in hyperosmolarity stressed human corneal epithelial cells and environment-induced dry eye patients. *Exp Eye Res*. 2015;134:133–140.
54. Zheng Q, Tan Q, Ren Y, et al. Hyperosmotic stress-induced TRPM2 channel activation stimulates NLRP3 inflammasome activity in primary human corneal epithelial cells. *Invest Ophthalmol Vis Sci*. 2018;59:3259–3268.
55. Li S, Sun Y, Song M, et al. NLRP3/caspase-1/GSDMD-mediated pyroptosis exerts a crucial role in astrocyte pathological injury in mouse model of depression. *JCI Insight*. 2021;6:e146852.
56. Lian H, Fang X, Li Q, et al. NLRP3 inflammasome-mediated pyroptosis pathway contributes to the pathogenesis of candida albicans keratitis. *Front Med*. 2022;9:845129.
57. Ibrahim MM, Maria DN, Mishra SR, Guragain D, Wang X, Jablonski MM. Once daily pregabalin eye drops for management of glaucoma. *ACS Nano*. 2019;13:13728–13744.
58. De Saint Jean M, Brignole F, Bringuier AF, Bauchet A, Feldmann G, Baudouin C. Effects of benzalkonium chloride on growth and survival of chang conjunctival cells. *Invest Ophthalmol Vis Sci*. 1999;40:619–630.
59. Noecker R. Effects of common ophthalmic preservatives on ocular health. *Adv Ther*. 2001;18:205–215.
60. Kanno S, Hirano S, Kato H, Fukuta M, Mukai T, Aoki Y. Benzalkonium chloride and cetylpyridinium chloride induce apoptosis in human lung epithelial cells and alter surface activity of pulmonary surfactant monolayers. *Chem -Biol Interact*. 2020;317:108962.
61. Green JP, Yu S, Martin-Sanchez F, et al. Chloride regulates dynamic NLRP3-dependent ASC oligomerization and inflammasome priming. *Proc Natl Acad Sci USA*. 2018;115:E9371–E9380.
62. Li S, Li H, Zhang YL, et al. SFTSV infection induces BAK/BAX-dependent mitochondrial DNA release to trigger NLRP3 inflammasome activation. *Cell Rep*. 2020;30:4370–4385 e7.
63. Zhang Y, Jiao Y, Li X, et al. Pyroptosis: A new insight into eye disease therapy. *Front Pharmacol*. 2021;12:797110.
64. Chen H, Gan X, Li Y, et al. NLRP12- and NLRC4-mediated corneal epithelial pyroptosis is driven by GSDMD cleavage accompanied by IL-33 processing in dry eye. *Ocul Surf*. 2020;18:783–794.
65. Luo L, Nguyen D, Huang C, Lai J. Therapeutic hydrogel sheets programmed with multistage drug delivery for effective treatment of corneal abrasion. *Chem Eng J*. 2022;429:132409.
66. Luo L, Nguyen D, Lai J. Long-acting mucoadhesive thermogels for improving topical treatments of dry eye disease. *Mater Sci Eng C Mater Biol Appl*. 2020;115:111095.
67. Nguyen D, Luo L, Lai J. Thermogels containing sulfated hyaluronan as novel topical therapeutics for treatment of ocular surface inflammation. *Mater Today Bio*. 2022;13:100183.
68. Lin P, Jian H, Li Y, et al. Alleviation of dry eye syndrome with one dose of antioxidant, anti-inflammatory, and mucoadhesive lysine-carbonized nanogels. *Acta Biomater*. 2022;141:140–150.